EVAPOTRANSPIRATION ESTIMATION OVER PASTURES IN CHILE FOR DROUGHT MONITORING

I.Moletto-Lobos, C. Mattar

University of Aysén, Obispo Vielmo 62, Coyhaique, italo.moletto@uaysen.cl; cristian.mattar@uaysen.cl

ABSTRACT

During the last decades, irrigation systems for pastures have been presented as a potential tool for paddock management, although evapotranspiration retrievals are still an asset and for preventing drought events. Thus, ET is a key parameter for determine water consumption of crops. In this work, we presented an evaluation of satellite-based models of pastures in the south of Chile. Datasets were setted up using remote sensing, automatic weather station and land surface cover maps. Four Surface Energy Balance (SEB) methods was calibrated: SEBS, SEBAL, METRIC and SSEBop for Actual Evapotranspiration (ET_a) estimates. The SSEBop and SEBS show the best results such as *RMSE* equal to 0.74 and 1.1 mm day^{-1} respectively. This work contributes to complement the information of the prairies water footprint and irrigation scheduling using ET_a satellite-based models for pastoral systems of Chile.

Key words — Evapotranspiration, Remote Sensing, Pastures, Chile, Landsat.

1. INTRODUCTION

The Evapotranspiration (ET) is a key parameter for estimate the water consumption of grazing grasslands to determinate the amount of irrigation and water footprint of pastoral systems [1,2]. The relevance of calculate the water consumption lies to adapt the water management of grassland on the phenological state and avoid climatic variation associated to the precipitation amount.

Remote sensing is an economic and efficient technique for spatially contiguous and frequent information of actual evapotranspiration (ET_a) retrievals, based on surface energy balance models (SEB). These models can be categorized as single layer, two-layer, two-patch, dual-source, multi-patch and multi-layer models [3]. Single layers models have been widely used to estimate ET_a at regional scale, such as SEBAL, METRIC, SEBS and SSEBop [4,5,6,7].

In Chile, the largest grazed grassland is in southern zone (-39°, -43.5°) where feeds 1.66 million heads of cattle [8]. The ET of this surface depends mainly on rainfall precipitation, especially during spring and summer [9]. In this context, the pastoral systems of south of Chile could be in vulnerability, due to the decrease in precipitation amount during the last decade, generating severe events of meteorological droughts [10,11].

Mixed evaluation of remote sensing models led determinate which model is adequate to estimate evapotranspiration over study area [12,13,14].
These models have not been applied in pastures in the southern zone of Chile and quantify the real needs of irrigation in pastoral systems. Therefore, the aim of this work is evaluating the ET_a performance using four SEB models (SEBS, SEBAL, METRIC and SSEBop) generated from remote sensing.

2. MATERIAL AND METHODS

2.1. Study Area and dataset

The study area is the temperate grasslands southern of Chile located between Los Ríos and Los Lagos Region (Figure 1). This area covers 1.32 million hectares of grasslands, where the average temperature is 10°C with an annual rainfall of 2100 mm [15]. The dataset used was Landsat 7 and 8 images for the period 2014-2017. Also, auxiliary data was used such as the Land Cover of Chile [16], SRTM Digital elevation model, the ASTER GED [17], atmospheric input for Land Surface Temperature calibration derived from Barsi Calculator [18] and agrometeorological stations for meteorological estimations. The Oromo Calibration Site (OCS) was used for validating the ET data [19].

2.2. Methods

Satellite based evapotranspiration models was based on surface energy balance equation:

$$R_N = H + \lambda E + G_0$$

Where R_N is net radiation, H the sensible heat flux, λE the latent heat flux and G_0 the soil heat flux. R_N was calibrated based on the surface radiation balance equation at the satellite overpass:

$$R_N = (1 - \alpha)\, R_{swd} + \varepsilon_\lambda R_{lwd} - \varepsilon_\lambda \sigma T_s^4$$

Where α is surface albedo estimated from Liang [20], R_{swd} is the descending shortwave radiation estimated based on Bristow-Campbell method [21], ε_λ is the surface emissivity derived from ASTER GED dataset, R_{lwd} is the long-wave descending radiation, σ is the Boltzmann constant and T_s correspond to the surface temperature estimated with single-channel method, were the parameters are detailed in [22,23]:

$$T_s = \gamma[\frac{1}{\varepsilon_\lambda}(\psi_1 L_{sen} + \psi_2) + \psi_3] + \delta$$

Where L_{sen} is the radiance in the thermal spectrum. $\psi 1$, $\psi 2$ and $\psi 3$ are atmospherics functions derived from the atmospheric radiance and transmissivity. γ and δ are parameters which depends on L_{sen} and the brightness temperature of sensor (Tb).

The sensible heat flux and latent heat flux was estimated based on SEBS, SEBAL, METRIC and SSEBop models. The soil heat flux was considered negligible for daily estimations [24].

SEBS model uses meteorological data and information from remote sensing based on the heat fluxes estimation under extreme condition using the Monin-Obukhov Similiarity

$$\Lambda_r = 1 - \frac{H - H_{wet}}{H_{dry} - H_{wet}}$$

Where Λ_r is the relative evaporative fraction, H_{wet} and H_{dry} are the sensible heat flux under wet and dry conditions respectively.

SEBAL and METRIC are physical models which estimates H by the parametrization of the vertical difference between aerodynamic temperature and air temperature close to the surface (dT) assuming the existence of a linear relationship between T_s and dT

$$H = \rho C_p \frac{dT}{r_{ah}}$$

This calibration uses the selection of anchor pixels for each image under exteme conditions (dry and wet) and the estimation of aerodynamic resistance (r_{ah}). For SEBAL, the cold pixel was H_{cold}=0 for water bodies or irrigated fields, and METRIC the selection of the cold pixel was based on irrigated alfalfa field (ET_r=1.05ET_0). For scaling instantaneous λE to daily ET_a values was used the method proposed by Sobrino, 2007 to scale the instantaneous R_N to daily R_N values [25].

The SSEBop model estimates ET_a from ET_0, the evaporative fraction (Λ) based on T_s, and a coefficient k that scales the grass reference experienced into maximum ET by an aerodynamically rougher crop.

$$ET_a = \Lambda k ET_0$$

The ET_a models estimated using Landsat imagery was compared with Adjusted crop evapotranspiration ($ET_{c\ adj}$) [26] measured at OCS through different statistical indicators. These statisical indicators used was the coefficient of determination (R^2), root mean square error ($RMSE$), relative root mean square error ($RRMSE$), the standard deviation of the residual values (σ) and the mean absolute error (MAE).

3. RESULTS

ET_a models derived from remotely-sensed data are shown at Figure 2 for summer days in the study area, where there is spatial variability according to the SEB model. SEBS and SSEBop model shows similar spatial patterns of evapotranspiration over the images. In February 13, 2015 at the center of image, east of Oromo the ET_a reaches values near to 0. During the summer of 2016, the water consumption increases and the whole grasslands presents homogeneous distribution (standard deviation: 0.86 mm day^{-1} SSEBop, 0.87 SEBS mm day^{-1}) of ET_a, with an average value of 5.59 mm day^{-1} for SSEBop and 5.79 mm day^{-1} for SEBS. During March 6, 2017 a lower evapotranspiration, principally at the southern area, due to the low R_n values. SEBAL depends on the selection of hot and cold pixels for ET_a computation, and the spatial patterns are similar for 15 Feb 2015 and 6 Mar 2017 in comparison with SEBS and SSEBop, SEBAL understimates low values of evapotranspiration and overestimate for higher variability with a standard deviation of 2.27 mm day^{-1}. METRIC shows a spatial variability due to the selection of anchor pixels over all imagery of Figure 3, such the image of 13 February,2017 METRIC estimated a very heterogeneous value (standard deviation: 2.49 mm day^{-1}) of ET_a for the whole area, where it coincides with the warmest Ts pixels and lowest R_N values.

This behavior shows over the remote sensing-based ET_a with a seasonal variability (Figure 3). SEBS shows a well performance with R^2 of 0.74, $RMSE$ 1.1 mm day^{-1}, $RRMSE$ of 45.17% and MAE of 0.92 mm day^{-1} (Figure 4) however, tends to overestimate the ET_a where the water consumption increases, especially for summer days during the meteorological drought years (2015-2016) for the southern grasslands [11,12], reaching an mean evaporative fraction of 0.78 for the summer period. The ET_a values estimated by the SSEBop model have a similar behavior to Oromo data, with R^2: 0.76, $RMSE$: 0.75 mm day^{-1}, MAE: 0.6 mm day^{-1} and $RRMSE$: 28.02%, so SSEBop presents a good fit. SEBAL, on the other hand, present a poor adjustment (R^2: 0.53) because it presents a high dispersion data, overestimating and underestimating extreme values during spring and summer (σ: 1.6 mm day-1), $RMSE$: 1.8 mm day-1, MAE: 1.6 mm day^{-1} and $RRMSE$: 62.89%. It is possible that dispersion of ET_a values is related to the selection of hot and cold pixels, with a high contrast of landscape conditions and presence of clouds. For example, the image of December 3, 2014, 22 and 30 November 2016 the cloud cover reaches up to 70%, so SEBAL overestimate the ET_a to the limitations of the model. METRIC does not present a correlation with the measured data of our station with R^2= 0.05, so the values estimated by METRIC do not represent the ET_a of the study area, the cause of the calibration of this model is possibly due to the same limitation presented by SEBAL.

4. DISCUSSION

The SSEBop (R^2: 0.75, $RMSE$: 0.75 mm day^{-1}) and SEBS (R^2: 0.74, $RMSE$: 1.1 mm day^{-1}) model were consistent with data estimated in Oromo. This adjustment is because SSEBop and SEBS does not solve the dT under the manual selection of anchors pixels. The models SEBAL (R^2: 0.53, $RMSE$: 1.8 mm

day^{-1}) and METRIC (R^2:0.05, *RMSE*: 2 mm day^{-1}) require the selection of extreme condition to estimate H and λE manually, where does not had a good performance over temperate grasslands of Chile. Thus, there is a limitation in SEBAL and METRIC model because requires clear sky images, a condition that does not happen frequently over study area, condition which could affect the parametrization of H. The results of SEBS validation presents a linear adjustment with 74% and *RMSE* of 1.1 mm day^{-1}, being a good model for ET_a estimation, however the higher ET values shows an overestimation in comparison with OCS.

5. CONCLUSIONS

In the present study, four SEB models was evaluated for ET_a estimation in grassland over Los Rios and Los Lagos regions using remote sensing and meteorological data. This was done through the processing satellite and meteorological database over the study area, information needed as input to modeling actual evapotranspiration of the different SEB models, which were validated with *in-situ* data. SSEBop turned out to be the model with best linear fit and lowest error compared with in-situ data (R^2: 0.75, *RMSE*: 0.75 mm day^{-1}) and SEBS the second model with acceptable performance (R^2: 0.74, *RMSE*: 1.1 mm day^{-1}), so these algorithms can be applied to estimate ET_a over grassland of pastoral systems of southern Chile. Finally, this work contributes to an estimate of actual water footprint of pastoral systems, a tool that contributes to the generation of land management plans that allow a sustainable and efficient use of water for drought monitoring.

6. REFERENCES

[1] S. Rost, D. Gerten, A. Bondeau, W. Lucht, and J. Rohwer, "Agricultural green and blue water consumption and its influence on the global water system," vol. 44, pp. 1–17, 2008.

[2] M. A. Zonderland-Thomassen, M. Lieffering, and S. F. Ledgard, "Water footprint of beef cattle and sheep produced in New Zealand: water scarcity and eutrophication impacts," J. Clean. Prod., vol. 73, pp. 253–262, 2014.

[3] K. Zhang, J. S. Kimball, and S. W. Running, "A review of remote sensing based actual evapotranspiration estimation," Wiley Interdiscip. Rev. Water, vol. 3, no. 6, pp. 834–853, 2016.

[4] Z. Su, "The Surface Energy Balance System (SEBS) for estimation of turbulent heat fluxes," Hydrol. Earth Syst. Sci., vol. 6, no. 1, pp. 85–100, 2002.

[5] W. G. M. Bastiaanssen et al., "A remote sensing surface energy balance algorithm for land (SEBAL).," J. Hydrol., vol. 212–213, pp. 213–229, 1998.

[6] R. G. Allen et al., "Satellite-Based Energy Balance for Mapping Evapotranspiration with Internalized Calibration (METRIC)—Applications," J. Irrig. Drain. Eng., vol. 133, no. 4, pp. 395–406, 2007.

[7] G. B. Senay et al., "Operational Evapotranspiration Mapping Using Remote Sensing and Weather Datasets: A New Parameterization for the SSEB Approach," J. Am. Water Resour. Assoc., vol. 49, no. 3, pp. 577–591, 2013.

[8] ODEPA, Boletín de carne bovina. Santiago, 2018.

[9] P. G. Flores, I. López, P. Kemp, and J. Dörner, "Sustainable Pasture Improvement in the South of Chile," Adv. Plants Agric. Res., vol. 6, no. 6, pp. 5–7, 2017.

[10] J. P. Boisier, R. Rondanelli, R. Garreaud, and F. Muñoz, "Anthropogenic Contribution to the Southeast Pacific Precipitation Decline and Recent (2010-2015) Mega-Drought in Chile," Am. Geophys. Union, Fall Meet. 2015, Abstr. id. H43E-1549, vol. 43, pp. 1–9, 2016.

[11] R. D. Garreaud, "Record-breaking climate anomalies lead to severe drought and environmental disruption in western Patagonia in 2016," Clim. Res., vol. 74,, no. 3, pp. 217–229, 2018.

[12] N. Bhattarai, S. B. Shaw, L. J. Quackenbush, J. Im, and R. Niraula, "Evaluating five remote sensing based single-source surface energy balance models for estimating daily evapotranspiration in a humid subtropical climate," Int. J. Appl. Earth Obs. Geoinf., vol. 49, pp. 75–86, 2016.

[13] Y. Chen et al., "Comparison of satellite-based evapotranspiration models over terrestrial ecosystems in China," Remote Sens. Environ., vol. 140, pp. 279–293, 2014.

[14] R. Singh and G. Senay, "Comparison of Four Different Energy Balance Models for Estimating Evapotranspiration in the Midwestern United States," Water, vol. 8, no. 1, p. 9, 2015.

[15] P. Sarricolea, M. Herrera-Ossandon, and Ó. Meseguer-Ruiz, "Climatic regionalisation of continental Chile," J. Maps, vol. 13, no. 2, pp. 66–73, 2017.

[16] Y. Zhao et al., "Detailed dynamic land cover mapping of Chile: Accuracy improvement by integrating multi-temporal data," Remote Sens. Environ., vol. 183, pp. 170–185, 2016.

[17] G. C. Hulley, S. J. Hook, E. Abbott, N. Malakar, T. Islam, and M. Abrams, "The ASTER Global Emissivity Dataset: Mapping Earth's emissivity at 100 meter spatial scale," Geophys. Res. Lett., vol. 42, no. 19, pp. 7966–7976, 2015.

[18] J. A. Barsi, J. L. Barker, and J. R. Schott, "An Atmospheric Correction Parameter Calculator for a single thermal band earth-sensing instrument," IGARSS 2003. 2003 IEEE Int. Geosci. Remote Sens. Symp. Proc. (IEEE Cat. No.03CH37477), vol. 5, no. C, pp. 3014–3016, 2003.

[19] C. Mattar et al., "The LAB-Net Soil Moisture Network: Application to Thermal Remote Sensing and Surface Energy Balance," Data, vol. 1, no. 1, p. 6, Jun. 2016.

[20] S. Liang et al., "Narrowband to broadband conversions of land surface albedo: I. Algorithms," Remote Sens. Environ., vol. 76, no. 1, pp. 213–238, 2000.

[21] K. L. Bristow and G. S. Campbell, "On the relationship between incoming solar radiation and daily

maximum and minimum temperature," Agric. For. Meteorol., vol. 31, no. 2, pp. 159–166, 1984.
[22] J. C. Jiménez-Muñoz, J. A. Sobrino, D. Skokovi´, C. Mattar, and J. Cristóbal, "Land surface temperature retrieval methods from Landsat-8 thermal infrared sensor data," Geosci. Remote Sens. Lett. IEEE, vol. 11, no. 10, pp. 1840–1843, 2014.
[23] J. C. Jímenez-Muñoz, J. A. Sobrino, J. Cristóbal, G. Sòria, M. Ninyerola, and X. Pons, "Obtención de la temperatura de la superficie terrestre a partir de la serie histórica LANDSAT Land surface temperature retrieval from," Rev. Teledetección, vol. 33, pp. 53–63, 2010.
[24] W. P. Kustas, C. S. T. Daughtry, and P. J. Van Oevelen, "Analytical treatment of the relationships between soil heat flux/net radiation ratio and vegetation indices," Remote Sens. Environ., vol. 46, no. 3, pp. 319–330, 1993.
[25] J. A. Sobrino, M. Gómez, J. C. Jiménez-Muñoz, and A. Olioso, "Application of a simple algorithm to estimate daily evapotranspiration from NOAA-AVHRR images for the Iberian Peninsula," Remote Sens. Environ., vol. 110, no. 2, pp. 139–148, 2007
[26] R. Allen, L. S. Pereira, D. Raes, and M. Smith, FAO Irrigation and Drainage Paper No. 56 - Crop Evapotranspiration, vol. 56. 1998.

7. ILLUSTRATIONS, GRAPHS AND PHOTOGRAPHS

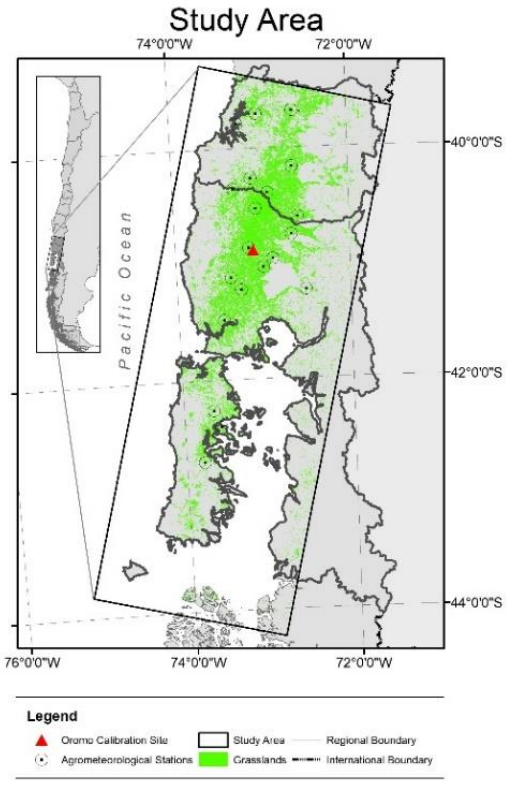

Figure 1. Study Area.

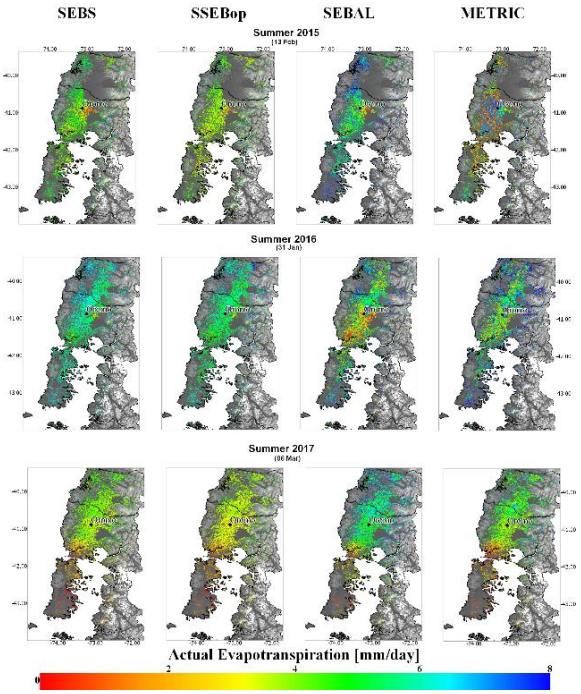

Figure 2. ETa maps for grassland cover for the spring-summer period of the study area, maps present zones without information over grassland cover due to the presence of clouds.

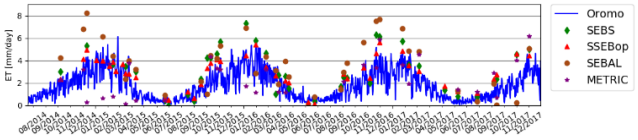

Figure 3. ET Time Series over Oromo Calibration Site. The blue line represents $ET_{c\ adj}$ estimated in Oromo, and points ET_a estimated by SEB models.

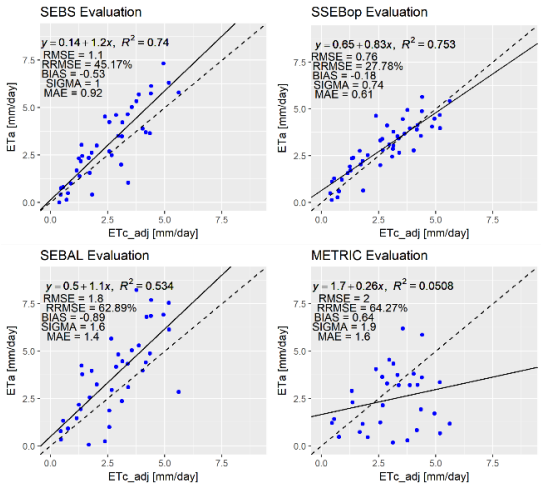

Figure 1. Evaluation of SEB models on Oromo. The dashed line represents the identity function and the continuous line shows the linear regression of each model.